A171

Multifunctional theranostic contrast agent for ultrasound and photoacoustic image guided tumor therapy with Focused Ultrasound triggered local delivery

Hyungwon Moon[1], Jeeun Kang[2], Changbeom Sim[2], Jin Ho Chang[2], Hyuncheol Kim[2], Hak Jong Lee[1]
[1]Seoul National University Bundang Hospital, Seongnam, Republic of Korea; [2]Sogang University, Seoul, Republic of Korea
Journal of Therapeutic Ultrasound 2016, **4(Suppl 1):**A171

Objectives
Not released for publication
Methods
Not released for publication
Results
Not released for publication
Conclusions
Not released for publication

A172

Low intensity ultrasound and microbubbles increase cellular cisplatin and enhances cisplatin effect in a bladder cancer mimicking culture model

Noboru Sasaki, Mitsuyoshi Takiguchi
Hokkaido University, Sapporo, Hokkaido, Japan
Journal of Therapeutic Ultrasound 2016, **4(Suppl 1):**A172

Objectives
Multi-modality treatment for muscle invasive bladder cancer aims selective organ preservation with favorable outcome. Cisplatin-based chemotherapy has a survival benefit in combination with radiotherapy. Local delivery of cisplatin may improve local disease control and survival rates. Ultrasound triggered microbubble cavitation enhances chemotherapeutic agents including cisplatin both *in vitro* and *in vivo*. However, it is not fully elucidated whether the enhancement is related to cisplatin concentration in tumor cells. The purpose of this work is to clarify the relation between enhanced cisplatin effect and cellular cisplatin concentration in a 3D culture system.
Methods
Human urinary bladder cancer cells were mixed with collagen type-I and were seeded into a culture dish at the volume of 50, 100, and 200 microL (Fig. 192). The gel mixture was exposed to non-focused ultrasound (center frequency 1 MHz, duty factor 50 %, intensity 0.9 mW/cm2, time 1 min) in the presence of cisplatin and microbubbles. For platinum measurement, cells were harvested from the gel right after the sonication and were separated from the dissolved gel. Cisplatin concentration was determined by measuring 195Pt with an inductively coupled plasma mass spectrometer. For assessing cell viability, cells were culture for 4 days in the gel after the sonication; thereafter cells were harvested and counted manually.
Results
The combination of ultrasound and microbubbles increased the cellular platinum concentration at all tested gel volume. Ultrasound alone did not significantly increase the cellular platinum concentration. Sonication did not increase the platinum concentration of the dissolved gel (i.e. without cells). The platinum concentration of the dissolved gel increased with the gel volume. The enhanced cytotoxic effect was observed at the gel volumes of 50 and 100 microL.
Conclusions
This study shows the feasibility of our culture model for assessing the relation of the intracellular delivery and the cytotoxic effect. With our ultrasound parameter, ultrasound-triggered microbubble cavitation has a potential to deliver cisplatin to cancer cells. Meanwhile, the results of this study suggest cisplatin in the extracellular matrix gradually enters cells and shows the cytotoxic effect even without ultrasound. Because cisplatin is a small molecular hydrophilic drug, it rapidly diffuses and may remain in the collagen. The thicker gel retained the higher platinum concentration. Further studies on ultrasound parameter may improve efficiency of the intracellular delivery and contribute to the local delivery of cisplatin in bladder cancer treatment.

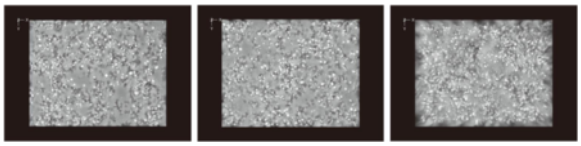

Fig. 192 (abstract A172). Microscopic images of the 3D model. Bladder cancer cells are embedded into collagen type-I. left, 50 microL; middle 100 microL; right 200 microL

A173

Model predictive control algorithm for large-area regional hyperthermia

Lukas Sebeke[1], Xi Luo[2], Bram de Jager[2], Maurice Heemels[2], Edwin Heijman[3], Holger Grüll[2]
[1]Uniklinik Koeln, Cologne, Germany; [2]Eindhoven University of Technology, Eindhoven, Netherlands; [3]Philips Research, Eindhoven, Netherlands
Journal of Therapeutic Ultrasound 2016, **4(Suppl 1):**A173

Objectives
Hyperthermia has been shown in clinical trials to strongly enhance therapeutic efficacy of radio- and chemotherapy. Main challenge in hyperthermia is to achieve temperatures between ca. 41-43 oC for ca. one hour. While current RF-based hyperthermia devices allow heating of larger volumes, they cannot heat specific subvolumes that are colder due to perfusion. HIFU has been used in preclinical and recently also in a clinical study for hyperthermia applications. The typical approach is to scan the focus point through the tissue using a real-time MRI thermometry feedback for temperature control (MR-HIFU). Here, we are currently developing a new regulatory algorithm based on Model Predictive Control (MPC) for stable HIFU-hyperthermia, which is designed to predict the temperature evolution under the influence of perfusion and diffusion inside the tissue and to plan a power application pattern, which will keep the temperature distribution within a predefined set of parameters.
Methods
The MPC algorithm aims to heat the target tissue to a predefined temperature profile using a heating model derived from the bioheat equation. A system of partial differential equations (PDE) is generated by transferring the heat equation to the Fourier domain. This PDE system is then used by the MPC algorithm to calculate the temperature distribution in the next timestep. The actual MR temperature readout functions as feedback for controlling the heating power (Fig. 193).
The control objective is to minimize the cost function of the soft constraints imposed on the temperature distributions. Their violation occurs if the modeled temperature doesn't fit in between the temperature profiles representing the maximum and minimum desired temperatures (Fig. 194). The algorithm was implemented with the Python interface of Gurobi.
To test the model, the predicted heating pattern was compared with MR-thermometry data acquired during sonications performed in a polyacrylamide phantom using the following HIFU-parameters: cell diameter 14 mm, time 45 s and power 30 W. A pixel-wise comparison was made between the acquired sagittal temperature maps and the modeled temperature per time step.
Results
First, the temperature diffusion terms of the PDE system were determined by fitting our model to the cooling curve of a test measurement. The pixel-wise temperature difference between the measurement temperature profile in the phantom and the model's prediction are shown in Fig. 195 as a boxplot in time, enabling us to see tendencies of over- or underestimation in the predictions. The whiskers were chosen to represent the range in which 90 % of the measurements lie. The upshifted boxes reveal that the model slightly overestimates most of the temperature values for the subsequent temperature distribution during the heating phase. Comparing the reach of the upper and the lower whiskers, we also see that under-estimations mostly stay below 0.4 °C, while over-estimations mostly stay below 0.8 °C. It follows that

the algorithm, using the model in its current implementation, will have a tendency to under-treat rather than to cause immediate thermal damage. It also reveals that the algorithm would benefit from a refined mechanism for online-adjustment of the heating estimation.

Conclusions

We have implemented the basic functionalities of a MPC-based algorithm for hyperthermia using HIFU. Given a treatment region and a safety margin, it computes a HIFU treatment sequence which meets the minimum required treatment temperature while respecting a given maximum temperature to avoid thermal damage. Using the model in its current implementation, the algorithm will likely have a tendency to under-treat rather than causing thermal damage as temperature estimation errors are more extreme in over-estimations.

We have yet to prove the viability of the algorithm in an experiment which uses the algorithm to steer the transducer. The good agreement between a real temperature development and the used model's prediction, however, gives us reason to believe that we will be able to present the working prototype of an MPC-based HIFU hyperthermia system in the near future.

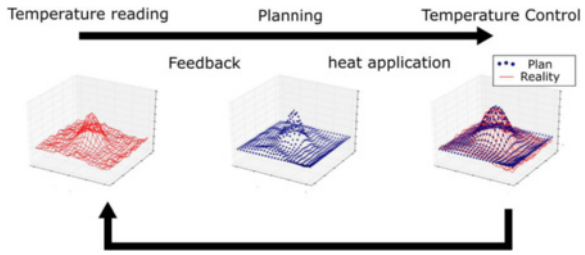

Fig. 193 (abstract A173). The information of the MR-thermometry image is used as feedback for the control algorithm to plan a heating pattern. The first of these heating steps is applied to control the temperature and a new measurement is taken

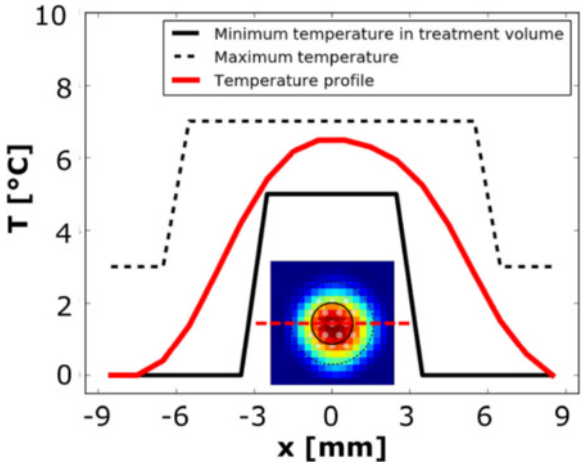

Fig. 194 (abstract A173). Scheme of Temperature thresholds given to the algorithm (black) and one possible temperature distribution outcome (red). Heatmap inset shows reading line for temperature profile displayed in graph and possible application points

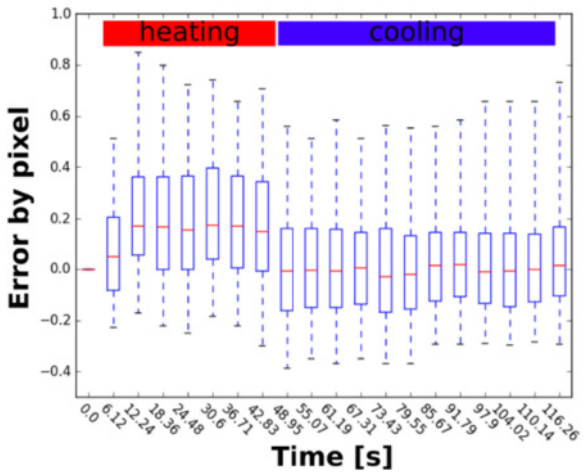

Fig. 195 (abstract A173). Boxplots of pixel-wise differences between experimental data and the model's prediction as boxplot versus the measurement time. Whiskers show the 90th percentile

A174

Image-based spatial HIFU transducer calibration for MRgFUS

Jan Strehlow[1], Michael Schwenke[1], Daniel Demedts[1], Tobias Preusser[1,2]
[1]Fraunhofer MEVIS, Bremen, Germany; [2]Jacobs University Bremen, Bremen, Germany

Journal of Therapeutic Ultrasound 2016, **4(Suppl 1):**A174

Objectives

In MRgFUS applications with movable transducers it is a common problem to establish a connection between scanner- and transducer-coordinate systems (spatial calibration). Vendor calibration tools are often only available in proprietary software and not accessible in research applications. Thus, transducer position and orientation are often prescribed in a tedious and error prone manual process. The current work presents an image-based spatial transducer calibration method that transforms a transducer model automatically into a given setup. Our method is based on the idea, that the water systems tubes are typically well visible in MR imaging and attached to one side of the transducer, giving information on the transducers position and orientation. An MR image of the transducer and its periphery can thus be used for an automatic calibration method.

Methods

Inputs for the method are an MR image of the transducer in a given setup and a transducer model. A transducer model consists of all relevant transducer information (such as e.g. transducer center, transducer orientation, or relative element positions) and a corresponding MR image. Note that this transducer model has to be established only once and can afterwards be used on any given setup. Both model- and setup-image should contain the transducer and its direct periphery, slice orientation should be roughly parallel to the transducer surface.

The transducer calibration is implemented as two-step process: An initialization is used to coarsely align setup and model image, a subsequent image registration aligns the images precisely. The accumulated transformation can then be used to map from transducer to MR coordinates and vice versa.

The initialization is a series of image registrations that subsequently align transducer to skin coupling, transducer center, and cable orientation.